T3-Tracer: A Tri-level Temporal-Aware Framework for Audio Forgery Detection and Localization

Shuhan Xia[1], **Xuannan Liu**[1], **Xing Cui**[1], **Peipei Li**[1]*

[1]Beijing University of Posts and Telecommunications, Beijing, China

Abstract

Recently, partial audio forgery has emerged as a new form of audio manipulation. Attackers selectively modify partial but semantically critical frames while preserving the overall perceptual authenticity, making such forgeries particularly difficult to detect. Existing methods focus on independently detecting whether a single frame is forged, lacking the hierarchical structure to capture both transient and sustained anomalies across different temporal levels. To address these limitations, We identify three key levels relevant to partial audio forgery detection and present T3-Tracer, the first framework that jointly analyzes audio at the frame, segment, and audio levels to comprehensively detect forgery traces. T3-Tracer consists of two complementary core modules: the Frame–Audio Feature Aggregation Module (FA-FAM) and the Segment-level Multi-Scale Discrepancy-Aware Module (SMDAM). FA-FAM is designed to detect the authenticity of each audio frame. It combines both frame-level and audio-level temporal information to detect intra-frame forgery cues and global semantic inconsistencies. To further refine and correct frame detection, we introduce SMDAM to detect forgery boundaries at the segment level. It adopts a dual-branch architecture that jointly models frame features and inter-frame differences across multi-scale temporal windows, effectively identifying abrupt anomalies that appeared on the forged boundaries. Extensive experiments conducted on three challenging datasets demonstrate that our approach achieves state-of-the-art performance.

Introduction

Advances in AI-generated content (AIGC) have led to unprecedented capabilities in audio synthesis(Li, Tang, and Liu 2024; Ma and Xia 2024; Bińkowski et al. 2019; Kim, Kim, and Yoon 2022; Ren et al. 2020). However, this progress also fuels a new wave of audio forgeries that threaten the credibility of information in fields such as media, law, and communications. Recently, content-driven partial audio forgery (Cai et al. 2022, 2024) has garnered attention as a particularly insidious variant. As shown in Fig.1(a), attackers modify critical frames or phrases to alter semantic meaning while preserving the overall acoustic authenticity of the audio, which greatly increases the difficulty of detection and forgery interval localization.

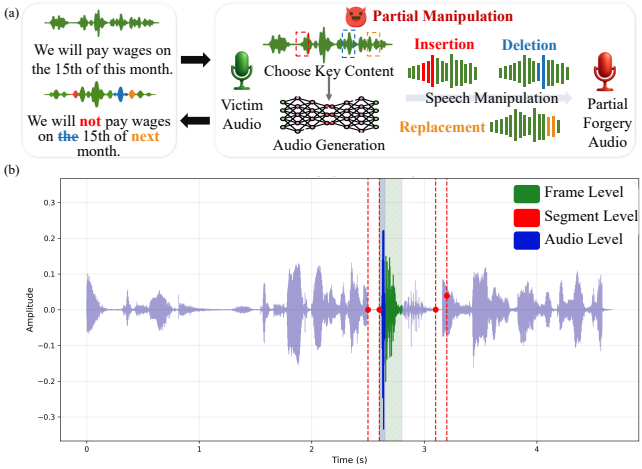

Figure 1: (a) The illustration of partial audio forgery generation, where subtle manipulations on key regions can lead to highly deceptive audio. (b) The manifestation of forged frames at different time levels. For example, forged frames show a large fluctuating envelope at the frame level, abnormal mutations at the segment level, and prominent amplitudes at the audio level.

In response to the growing threat of partial audio forgery, recent studies have introduced dedicated benchmarks(Cai et al. 2022; Zhang et al. 2023) and formalized two tasks: Partial Forgery Detection (PFD) and Temporal Forgery Localization (TFL). Among them, PFD formulates the problem as a single frame binary classification, and TFL is responsible for converting discrete frame classifications into continuous forged intervals and makes further corrections at the temporal intervals, which is usually through a linear regression head. Therefore, improving the detection accuracy of PFD is the key to solving the task of TFL.

Existing methods for partial forgery detection (PFD) can be broadly categorized into two types: frame forgery classification and boundary detection. The first type treats an audio sequence as a set of independent frames and classifies each frame based on anomalies in channel(Wu et al. 2024) or spectral features(Guo et al. 2024). While this ap-

*Corresponding authors

proach is intuitive and straightforward, it operates solely at the frame level, ignoring potential semantic inconsistencies that may emerge across wider temporal scales. Furthermore, frame-wise classification often results in scattered false positives, making it difficult to form coherent forged intervals in the subsequent temporal forgery localization (TFL) process. The second type aims to identify the start and end points of forged segments, typically using CNN(Cai et al. 2023) or temporal masking mechanisms(Xie et al. 2024). However, these methods still rely on per-frame predictions and lack explicit context modeling structures, making it difficult to capture abrupt transitional anomalies between boundary frames and their surrounding neighbors. This analysis demonstrates the importance of multi-scale temporal modeling in order to comprehensively capture the diverse characteristics of partial audio forgeries.

Based on extensive analysis of forged audio waveforms, as shown in Fig.1(b), we reveal three temporal levels relevant to partial audio forgery detection: frame, segment, and audio. The frame level refers to individual audio frames. The segment level refers a local window of frames centered around a target frame. And the audio level refers global context across the entire audio sequence. Forged content generated by AIGC may exhibit anomalies at each of these levels. **At the frame level**, forged frames often contain abnormal channel or spectral patterns. **At the audio level**, they may show global inconsistencies—such as mismatches in speaker identity, prosody, or background noise—when compared to authentic frames. **At the segment level**, transitional boundaries between real and forged regions often exhibit abrupt inconsistencies. These are reflected as abnormal mutation between the center frame and its neighboring context in a segment.

Motivated by these observations, we propose T3-Tracer, a multi-granularity temporal modeling framework for partial audio forgery detection and localization. T3-Tracer consists of two core and complementary modules: the Frame-Audio Feature Aggregation Module (FA-FAM) and the Segment-level Multi-Scale Discrepancy-Aware Module (SMDAM). FA-FAM focuses on frame forgery detection by aggregating both single frame acoustic features and global semantic context, providing multi-perspective features for each frame. SMDAM is designed for boundary detection. It employs a dual-branch structure to model both the original frame sequence and inter-frame differences, and applies attention mechanisms across multi-scale temporal segments to capture abrupt transitional anomalies near forged boundaries. In order to decrease scattered false positives frames, we integrates a cross-attention mechanism to explicitly fit the dependency between frame and boundary forgery cues, further improving detection robustness for PFD and localization accuracy for TFL. Our main contributions can be summarized as follows:

- We reveal three key levels relevant to partial audio forgery detection and propose T3-Tracer, a novel tri-level temporal-aware framework that comprehensively models audio forgery characteristics across frame, audio and segment levels. To our knowledge, this is the first work to systematically introduce multi-granularity temporal modeling for partial audio forgery detection and localization.
- We design two complementary modules: FA-FAM and SMDAM. FA-FAM operates at both the frame and audio levels and combine intra-frame forgery cues with global semantic inconsistencies to perform frame forgery detection. SMDAM focuses on the segment level, modeling both original frame features and inter-frame differences within multi-scale temporal segments to detect forgery boundaries.
- We conduct extensive experiments on three challenging datasets, demonstrating that T3-Tracer consistently outperforms state-of-the-art methods across various metrics and scenarios.

Related Work

Audio Forgery Detection

Audio forgery detection focuses on determining whether an input audio contains tampered or synthetic content. Early methods(Gomez-Alanis et al. 2020; Jung et al. 2022; Wang et al. 2022; Tak et al. 2021; Wu et al. 2023) in this domain primarily targeted utterance-level detection, aiming to distinguish fully generated or manipulated speech from genuine recordings. For instance, DARTS(Wang et al. 2022) proposed an end-to-end architecture composed of convolutional and residual blocks, which simultaneously learns deep speech representations and decision boundaries. ASDG(Xie et al. 2023) introduced a domain generalization framework that jointly optimizes feature aggregation and separation to improve robustness against unseen forgery types.

Although these methods achieve impressive performance in detecting entirely fake audio, they fall short when dealing with partially forged content. The Partial Forgery Detection (PFD) task requires finer temporal resolution to identify small-scale manipulations embedded within long-duration audio. To address this, recent studies have explored various detection granularities(Cai and Li 2024; Cai, Wang, and Li 2023; Li et al. 2023; Wu et al. 2022; Xie et al. 2024; Zhang et al. 2022; Zhu et al. 2023), ranging from segment-level to frame-level analysis. For example, QASAM(Wu et al. 2022) employed a question-answering framework to directly locate fake spans rather than relying on global shortcuts. TDL(Xie et al. 2024) introduced an embedding similarity module to separate real and fake frames in the representation space. PSDL(Zhang et al. 2022) and MGBF(Li et al. 2023) utilized self-supervised (SSL) front-end encoders and combined multi-resolution strategies to adapt to forgeries at different temporal scales. MFA(Guo et al. 2024) further refined SSL representations by dynamically pooling across multiple layers and aggregating them with a linear projection. IFBDN(Cai and Li 2024) designed a boundary-aware head to estimate the likelihood of each frame being near a forgery boundary.

However, most existing PFD approaches still inherit the fundamental paradigm of utterance-level detection, treating each frame as an isolated unit. While detection granularity

has improved, these methods largely overlook the temporal structure and semantic continuity across frames.

Temporal Forgery Localization

In recent years, temporal forgery localization (TFL) has received increasing attention in multimodal audio-visual forensics. Traditional tasks such as temporal anomaly detection(Zhou et al. 2024; Eldele et al. 2024) and action localization(Zhou et al. 2025; Zhang, Wu, and Li 2022) typically rely on distributional deviations or visually salient transitions. However, TFL focuses on identifying maliciously inserted short audio-visual spans that often imitate the local acoustic or visual patterns of surrounding frames. These characteristics make it difficult for existing solutions in those domains to handle subtle and sparse forgeries, underscoring the need for dedicated modeling strategies.

To address this challenge, LAV-DF(Cai et al. 2022) introduced the first content-driven multimodal TFL dataset and proposed the BATFD network, which detects forgery traces through a combination of a single-frame classification module and a boundary matching module. It uses a linear layer as a decoder to determine whether each frame is forged. The forged frame is then represented as a continuous forged interval according to the temporal resolution. Its follow-up work, BATFD+(Cai et al. 2023), added a boundary-sensitive network (BSN) for auxiliary boundary prediction and employed a multimodal fusion module to facilitate cross-modal interaction between audio and video. Building on this, AV-TFD(Liu et al. 2023) leveraged cross-modal attention to align audio and video representations at the encoding stage. UMMAFormer(Zhang et al. 2023) further enhanced the detection of subtle forgery cues by incorporating reconstruction learning, cross-reconstruction attention, and a parallel feature pyramid network, using ActionFormer as the decoder for localization.

While multimodal TFL can benefit from cross-modal inconsistencies to detect forgery traces, unimodal audio forgeries often rely on subtle manipulations—such as phoneme-level modifications—that preserve acoustic coherence but alter semantics. This subtlety increases the difficulty of accurate detection. CFPRF(Wu et al. 2024) was the first to formally define the audio TFL task, proposing a two-stage framework consisting of a frame-level detection network and a proposal refinement network. It proposes a new decoder PRN, which uses a verification head and a regression head to correct the coarse-grained proposals. Although the decoder performs well, its localization ability is still limited by the PFD task module.

Methodology

Overview

To detect and localize partial audio forgeries in long audios by capturing forgery cues at multiple temporal levels, we propose T3-Tracer, a unified framework that jointly analyzes audio at the frame, segment, and audio levels. The overall pipeline is illustrated in Fig.2 and consists of four main components: (1) Feature Encoder. The input audio waveform is first processed by a self-supervised speech encoder followed by CNN-based residual blocks, yielding enhanced frame-level acoustic features. (2) Frame–Audio Feature Aggregation Module (FA-FAM). FA-FAM aims to determine whether each frame has been forged from both the frame and audio perspectives. It first aggregates diverse anomaly patterns within frames, then captures long-range temporal inconsistencies across the entire audio. (3) Segment-level Multi-Scale Discrepancy-Aware Module (SMDAM). SMDAM divides temporal segments at multiple scales to detect temporal boundaries between real and forged regions, serving as a double check to optimize the classification results for a single frame. (4) Feature Fusion and Decoder. Finally, the forgery-aware features from FA-FAM and the boundary-aware features from SMDAM are fused via a cross-attention mechanism. We use PRN(Wu et al. 2024) as a decoder to produce forgery probabilities of each frame and converts them into continuous forged intervals for TFL while refining temporal boundaries.

Feature Encoder

Given the proven effectiveness of self-supervised speech models for downstream tasks, we adopt *Wav2Vec2-XLSR-300M*(Conneau et al. 2020) as our backbone to extract audio features. Specifically, we obtain 1024-dimensional embeddings from the final hidden states. To reduce computational complexity, we project these embeddings into a lower-dimensional feature space using a linear layer, yielding a feature map of shape $\mathbb{R}^{C\times T}$, where T denotes the number of audio frames and C is the reduced feature dimension.

Since the self-supervised learning (SSL) features are insufficient to model per-frame spectral and channel-level information, we follow CFPRF(Wu et al. 2024) and further enhance the representation via six CNN-based residual blocks. This enhancement transforms the feature map into a three-dimensional tensor $\mathbf{S} \in \mathbb{R}^{C\times T\times S}$, where C and S denotes channels and spectral bins for each frame.

Frame-Audio level Feature Aggregation Module

Existing frame forgery detection methods only focus on the frame level and lack global temporal context. To address this limitation, we propose the Frame–Audio Feature Aggregation Module (FA-FAM), which consists of two sequential components: Frame-level Feature Aggregation (FFA) to capture intra-frame fine-grained forgery cues, and Audio-level Feature Aggregation (AFA) to model global temporal inconsistencies.

Frame-level Feature Aggregation Since FA-FAM completes the frame forgery detection at both the frame level and the audio level, it is very important to design an excellent frame-level detection method. Existing researches have shown that different audio manipulation techniques exhibit distinct forgery characteristics. For example, delete some frames may exhibit unnatural spectral transitions(Zhang et al. 2025), while spliced segments often disrupt channel consistency(Xie et al. 2024). However, conventional detection methods usually rely on CNNs(Huang et al. 2025; Zou et al. 2024) or dynamic pooling(Guo et al. 2024) to coarsely distinguish between authentic and forged frames. This type

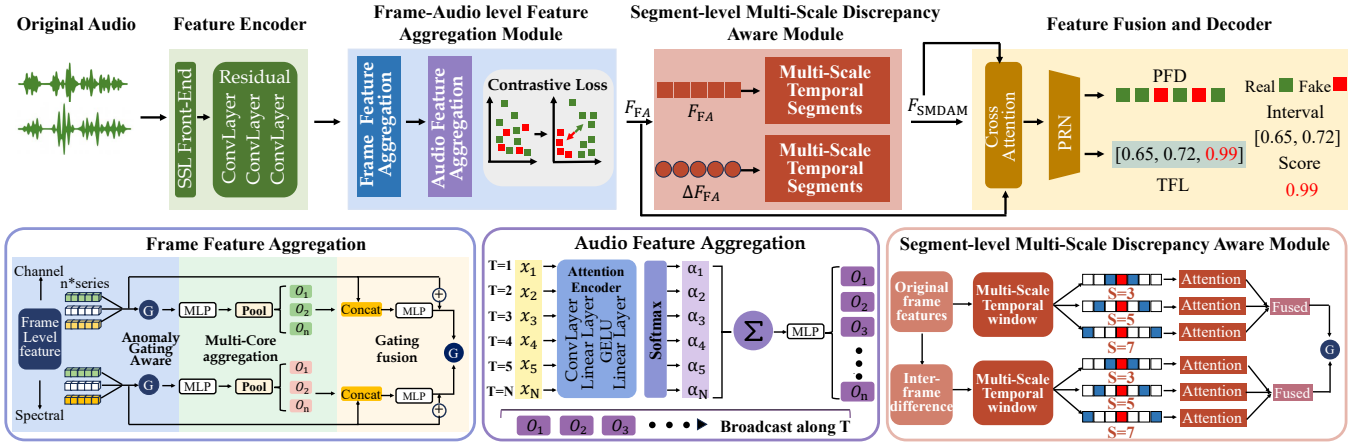

Figure 2: Overall pipeline of the proposed T3-Tracer **(top)** and detailed architecture of its key components **bottom**, including Frame–Audio Feature Aggregation Module (FA-FAM) with Frame Feature Aggregation and Audio Feature Aggregation, and Segment-level Multi-Scale Discrepancy-Aware Module (SMDAM).

of method treat all feature dimensions uniformly and thus overlook the diverse anomaly patterns introduced by different manipulation techniques.

To address this issue, FFA constructs a set of forgery-aware core vectors ("cores") along the channel and spectral dimensions, where each core is designed to capture a key representation of a different tampering pattern. Inspired by the aggregation mechanism of STAR(Han et al. 2024), we use an aggregation operator to instantiate these cores.

Specifically, given a frame-level feature map $s \in \mathbb{R}^{C\times T\times S}$ extracted from our feature encoder, we derive dimension-specific projections $s_c \in \mathbb{R}^{C\times T}$ and $s_s \in \mathbb{R}^{S\times T}$ for channel and spectral information, respectively. Within each dimension, we construct n forgery-aware cores $\{o_j\}_{j=1}^{n}$ that collectively fit the diverse forgery patterns. The core representation o_j is a vector generated by an arbitrary function f with the following form:

$$o_j = f(x_1, x_2, ..., x_N), \tag{1}$$

where $x_1, x_2, ..., x_N$ is a multivariate series with N channels or spectral bins.

Since forgery anomalies may not be uniformly represented across N dimensions, we design an anomaly gating aware mechanism that adaptively predicts the weight of each dimension in constructing the core, thereby emphasizing potential spurious anomalies while suppressing normal acoustic patterns. To obtain such representation, we employ the following form:

$$o_j = \text{Stoch\_Pool}_j(\text{MLP}_1(G \odot X)), \quad j = 1, ..., n \tag{2}$$

where X represents either s_c or s_s, $\odot$ denotes element-wise multiplication, G is the anomaly gating aware mechanism and Stoch_Pool_j is a stochastic pooling operation.

Subsequently, Each unit x_i is then enhanced by concatenating all cores $\{o_j\}_{j=1}^{n}$:

$$x_i' = \text{MLP}([x_i \| o_1 \| \ldots \| o_n]) + x_i, \tag{3}$$

here, the MLP is used to fuse the concatenated presentation and project it back to the hidden dimension. Like many other modules, we also add a residual connection from the input to the output. Finally, we adaptively integrate the enhanced channel and spectral representations through a learnable soft gating mechanism, which can determine the relative contribution of each dimension.

Audio level Feature Aggregation To capture global inconsistencies, we introduce the Atterance-level Feature Aggregation (AFA). While AFA adopts the same feature aggregation principle as FFA, it operates along the temporal dimension and employ a global attention mechanism to model dependencies between each frame and all others in the audio.

Specifically, given an input sequence $X \in \mathbb{R}^{T\times C}$ from FFA, AFA apply a lightweight attention encoder to compute normalized weights α for each frame:

$$\alpha = \text{softmax}(E_{\text{att}}(X)), \tag{4}$$

Using these weights, we derive a global context vector through a weighted sum over the sequence:

$$x_{\text{attn}} = \sum_{t=1}^{T} \alpha_t \cdot X_t, \tag{5}$$

This vector is subsequently projected through a MLP to yield the global core representation:

$$o_g = \text{MLP}(x_{\text{attn}}) \in \mathbb{R}^{d'}, g = 1, ..., n \tag{6}$$

The resulting global core is fused back with the original input via a gated residual connection, enhancing the model's ability to capture audio-level forgery patterns.

Segment-level Multi-Scale Discrepancy Aware Module

After completing forgery detection for individual frames, previous methods typically generate per-frame forgery prediction scores and input them directly to a decoder for the TFL task. However, relying solely on frame forgery detection often results in isolated false positive predictions. While

these scattered errors minimally impact PFD performance metrics, they significantly hinder the formation of coherent forged intervals during TFL, resulting in multiple incorrectly localized segments with extremely short durations. To complement FA-FAM and further enhance the reliability of frame forgery detection, we introduce the Segment-level Multi-Scale Discrepancy-Aware Module (SMDAM). Rather than directly classifying each frame, SMDAM focuses on identifying the temporal boundaries between authentic and forged segments, serving as a complementary signal to refine frame predictions.

Formally, given the feature sequence $F = \{f_t\}_{t=1}^{T}$, we define a set of temporal windows with different radii $\{k\}$ centered at each time step. For each scale k, we apply localized self-attention to capture contextual inconsistencies:

$$\tilde{f}_t^{(k)} = \text{Attn}^{(k)}(\mathcal{N}_k(f_t)), \tag{7}$$

where $\mathcal{N}_k(f_t)$ denotes the temporal neighborhood of frame t with radius k. This multi-scale design allows the module to detect boundary transitions occurring at different temporal spans.

To further highlight temporal variations, we introduce a difference branch that operates on inter-frame differences:

$$\delta_t = f_{t+1} - f_t, \quad \tilde{\delta}_t^{(k)} = \text{Attn}^{(k)}(\mathcal{N}_k(\delta_t)). \tag{8}$$

The original feature branch $\tilde{f}_t^{(k)}$ captures absolute inconsistencies, while the difference branch $\tilde{\delta}_t^{(k)}$ explicitly models abrupt changes. Their outputs are fused via a gated integration:

$$F_b = G \cdot \tilde{\delta}_t^{(k)} + (1 - G) \cdot \tilde{f}_t^{(k)}, \tag{9}$$

where the gate G is predicted from the concatenated features using a sigmoid-activated linear layer.

Finally, a fully connected layer converts the fused features into boundary probability scores $\hat{Y}_b = \{\hat{y}_b^1, \hat{y}_b^2, \ldots, \hat{y}_b^T\}$, which indicate the likelihood of each frame being a boundary between authentic and forged segments.

Feature Fusion and Decoder

To fully leverage the complementary information from FA-FAM and SMDAM, we employ a cross-attention mechanism to enhance the forgery-aware features using boundary-aware cues. Since the inputs are permutation-invariant, positional encodings $\text{PE}(\cdot)$ are added to both feature sequences to encode temporal ordering. We first compute a boundary-aware correlation map M_{attn} between the frame forgery features F_{FA} and the boundary detection features F_{SMDAM}. This is achieved by projecting the inputs into query and key representations:

$$Q = W_q\,\text{PE}(F_{\text{FA}}), \quad K = W_k\,\text{PE}(F_{\text{SMDAM}}), \tag{10}$$

and normalizing their dot product:

$$M_{\text{attn}} = \text{softmax}\left(\frac{QK^\top}{\sqrt{C}}\right), \tag{11}$$

To obtain the boundary-enhanced features, we project the forgery-aware features into the value space using W_v and apply the attention map:

$$V = W_v\,\text{PE}(F_{\text{FA}}), \quad F_{\text{ca}} = M_{\text{attn}}V. \tag{12}$$

The enhanced representation F_{ca} is then added back to the original forgery-aware features and passed through a feed-forward network with layer normalization to generate the fused boundary-aware representations F_{ba}. Finally, we adopt a PRN-based decoder to progressively refine and downsample the fused features F_{ba} across multiple temporal resolutions. The decoder produces the each frame forgery probability scores $\hat{Y}_f = \{\hat{y}_1^f, \hat{y}_2^f, \ldots, \hat{y}_T^f\}$, and simultaneously converts the discrete frame predictions into continuous forged intervals with accurate boundary localization for the TFL task.

Training and Inference

Our framework is optimized using frame loss, boundary loss and Contrastive Loss. The frame loss directly supervises the frame-level forgery probability score $\hat{Y}_f = \{\hat{y}_1^f, \hat{y}_2^f, \ldots, \hat{y}_T^f\}$ produced by the fusion and prediction module. We use a MSE loss with respect to the ground-truth labels Y_f:

$$\mathcal{L}_{\text{f}} = \frac{1}{T}\sum_{t=1}^{T}\text{MSE}(\hat{y}_t^f, y_t^f), \tag{13}$$

where $y_t^f \in \{0, 1\}$ denotes the forgery label of the t-th frame. To explicitly supervise the detection of forged segment boundaries, we apply an MSE loss to the boundary probability scores $\hat{Y}_b = \{\hat{y}_b^1, \hat{y}_b^2, \ldots, \hat{y}_b^T\}$ predicted by SMDAM:

$$\mathcal{L}_{\text{b}} = \frac{1}{T}\sum_{t=1}^{T}\text{MSE}(\hat{y}_t^b, y_t^b), \tag{14}$$

where $y_t^b \in \{0, 1\}$ is the ground-truth boundary label. To enhance feature discriminability in the FA-FAM, we employ a contrastive loss that encourages representations of frames from the same class to be close in the feature space, while pushing apart those from different classes. For the j-th pair of frames, the similarity is measured as:

$$SIM(f_a, f_b) = \frac{f_a^\top f_b}{\|f_a\|_2\|f_b\|_2}, \tag{15}$$

and the contrastive loss is defined as:

$$L_c = \frac{1}{J}\sum_{j=1}^{J}\big[I_j(1 - SIM(f_j, f_j^+))^2 + (1 - I_j)\max(0, SIM(f_j, f_j^-) - \alpha)^2\big], \tag{16}$$

where I_j=1 if the pair is from the same class and 0 otherwise, and α is a margin hyperparameter. The overall training objective is:

$$\mathcal{L} = \lambda_1\mathcal{L}_{\text{f}} + \lambda_2\mathcal{L}_{\text{b}} + \lambda_3\mathcal{L}_{\text{c}}, \tag{17}$$

where λ_1, λ_2,λ_3 balance the three loss terms.

During inference, we first obtain the frame forgery probability scores and continuous forged intervals from the PRN decoder. The results are then post-processed using the Soft-NMS(Bodla et al. 2017) technique to suppress predictions that are predicted to be in the same category but are highly overlapping.

Experiments

Experimental Setting

Datasets. We evaluate our method on three public datasets: LAV-DF(Cai et al. 2022), ASVS2019-PS(Zhang et al. 2022) (PS), and HAD(Yi et al. 2021). Among them, PS introduces multiple short forgery spans with diverse manipulation types, posing higher challenges.

Compared Methods. For PFD, we compare T3-Tracer with several state-of-the-art methods: PSDL (Zhang et al. 2022), IFBDN (Cai and Li 2024), and CFPRF. For TFL, we include both unimodal methods (PSDL, IFBDN, CFPRF) and multimodal methods (BA-TFD (Cai et al. 2022), BA-TFD+ (Cai et al. 2023), UMMAFormer (Zhang et al. 2023)) by using only audio input during inference to simulate unimodal performance.

Evaluation Metrics. Following CFPRF(Wu et al. 2024), we report Equal Error Rate (EER), Area Under the Curve (AUC), False Negative Rate (FNR), False Positive Rate (FPR), and F1-score for the PFD task. For TFL, we compute Average Precision (AP) at Temporal IoU thresholds $\{0.5, 0.75, 0.9, 0.95\}$, Average Recall (AR) at average proposal numbers $\{1, 2, 5, 10, 20\}$, and mean AP (mAP) over thresholds in the range $[0.5{:}0.05{:}0.95]$.

Implementation Details. All models are implemented using PyTorch and trained with a single NVIDIA GeForce RTX 3090 GPU. We adopt the Adam optimizer with a learning rate of $1e{-}7$, weight decay of $1e{-}4$, and train for 50 epochs with a batch size of 2. In our loss function, we set λ_1=1, λ_2=0.25 and λ_3=0.1. In the FA-FAM stage, we set the number of cores to 3. In the SMDAM stage, we set the multi-scale temporal segments to 3, 5, and 7.

Comparison and Analysis

Table 1: Partial forgery detection results. Performance comparison with state-of-the-art PFD methods on evaluated datasets using different evaluation metrics.

Dataset	Method	EER ↓	AUC ↑	Pre ↑	Rec ↑	F1 ↑
HAD	IFBDN	0.35	99.98	99.92	99.65	99.78
	PSDL	0.18	99.97	99.96	99.82	99.89
	CFPRF	0.08	99.96	99.98	99.92	99.95
	T3-Tracer	**0.07**	**99.98**	**99.98**	**99.92**	**99.95**
LAV-DF	IFBDN	1.07	99.88	99.94	98.93	98.93
	PSDL	0.82	99.92	99.95	99.18	99.57
	CFPRF	0.82	99.89	99.95	99.18	99.56
	T3-Tracer	**0.80**	**99.93**	**99.96**	**99.21**	**99.57**
PS	IFBDN	9.68	95.70	93.72	90.32	91.99
	PSDL	12.47	93.30	91.82	87.53	89.62
	CFPRF	7.50	96.95	95.18	92.50	93.82
	T3-Tracer	**7.41**	**97.13**	**95.32**	**93.46**	**94.04**

Partial Forgery Detection. We report the results of the PFD task in Table 1. Our proposed T3-Tracer consistently achieves the best performance across all three datasets. On the most challenging ASVS2019-PS, which contains frequent and short-span forgeries, T3-Tracer obtains an EER of 7.41% and an F1-Score of 94.04%. This highlights the effectiveness of our tri-level temporal modeling in capturing fine-grained forgery traces. While our framework is specifically designed to handle subtle and sparse audio manipulations, it also delivers consistent improvements on relatively less challenging benchmarks such as HAD and LAV-DF, with noticeable gains observed in both EER and F1. This indicates that the proposed approach maintains strong robustness across different levels of forgery difficulty.

Temporal Forgery Localization. We further evaluate T3-Tracer on the TFL task, with results summarized in Table 2. Our method achieves the best mAP on all three benchmarks. Specifically, T3-Tracer reaches mAP scores of 99.27%, 94.29%, and 57.28% and AR@1 scores of 99.33%, 87.79%, and 21.65% on HAD, LAV-DF, and PS datasets, respectively. Compared with existing audio TFL baselines such as IFBDN, PSDL, and CFPRF, our framework shows significant advantages, particularly on PS, which contains multiple short and overlapping forgery spans. This validates the effectiveness of our T3-Tracer for fine-grained boundary estimation. Compared with multimodal methods, BA-TFD and BA-TFD+ underperform when only audio is used. Although UMMAFormer shows reasonable performance on HAD and LAV-DF where forgeries are relatively long and isolated, its performance declines on PS and high-precision localization metric such as AP@0.95. This reveals its limited capacity for precise boundary detection and multi-segments localization.

Ablation Studies

Effectiveness of our core modules. To investigate the individual contributions of each temporal modeling component, we conduct ablation experiments by progressively removing the core modules from our proposed T3-Tracer. The results are summarized in Table 3. We observe that removing any one of the three modules leads to a consistent performance drop across all datasets and metrics, validating the necessity of temporal modeling at multiple granularities. Specifically, removing FFA causes a sharp decline in PFD, highlighting the importance of cross-channel and spectral feature aggregation for capturing fine-grained spatial anomalies. Excluding AFA impairs long-range temporal consistency modeling, which is particularly harmful on PS and LAV-DF datasets which use advanced forgery technology, and the features of a single frame are not enough to determine whether it is forged. Moreover, discarding SMDAM severely degrades boundary localization performance, especially on PS where densely packed forgery segments require precise detection of segment-level discontinuities. Finally, the combination of the three modules achieved the best results, indicating that their integration enables T3-Tracer to build a comprehensive temporal representation that is robust to different operation modes.

Ablation Study of the FA-FAM. We evaluate the core designs shared by the intra-frame and global modules, including the multi-core aggregation, anomaly-aware gating, and gated fusion strategy. Results are presented in Table 4. Removing the multi-core structure and use only a core leads to performance drops, especially on challenging datasets, showing its effectiveness in modeling diverse manipulation patterns. Disabling the anomaly-aware gate also degrades

Table 2: Temporal forgery localization result. Performance comparison with state-of-the-art TFL methods and PFD models.

Dataset	Method	AP@0.5	AP@0.75	AP@0.9	AP@0.95	mAP	AR@1	AR@2	AR@5	AR@10	AR@20
HAD	BA-TFD	79.86	37.98	5.55	0.57	40.93	45.12	47.53	49.99	52.09	55.15
	BA-TFD+	88.26	70.69	37.83	7.39	64.83	67.49	68.44	69.06	69.39	70.15
	UMMAFormer	**99.98**	**99.86**	98.01	88.17	98.49	98.68	98.73	98.84	98.85	98.86
	IFBDN	93.85	91.55	87.75	79.08	90.40	96.07	97.39	97.54	97.54	97.54
	PSDL	88.53	85.27	80.80	73.25	84.25	93.40	96.30	96.89	96.94	96.94
	CFPRF	99.77	99.60	99.21	96.03	98.65	99.31	99.38	99.38	99.38	99.38
	T3-Tracer	99.74	99.78	**99.43**	**96.33**	**99.27**	**99.33**	**99.46**	**99.46**	**99.46**	**99.46**
LAV-DF	BA-TFD	53.53	10.98	0.36	0.02	20.77	29.56	32.22	34.73	38.03	44.66
	BA-TFD+	83.78	51.99	6.13	0.46	49.32	52.78	54.97	57.21	58.41	60.04
	UMMAFormer	**97.29**	**95.67**	89.92	61.97	92.04	85.67	91.77	94.89	95.64	**96.14**
	IFBDN	86.83	84.02	77.85	70.09	82.55	86.28	91.78	92.13	92.13	92.13
	PSDL	76.10	71.71	65.16	57.13	70.43	84.71	89.14	89.98	90.03	90.03
	CFPRF	94.52	93.47	91.65	88.64	93.01	87.59	93.49	93.51	93.51	93.51
	T3-Tracer	94.70	93.82	**92.07**	**89.27**	**94.29**	**87.79**	**93.89**	**93.89**	**93.89**	95.89
PS	BA-TFD	13.65	4.91	1.06	0.63	6.15	8.04	11.03	15.41	19.14	23.64
	BA-TFD+	15.72	6.37	2.05	1.95	7.69	7.93	12.62	18.28	22.17	26.71
	UMMAFormer	52.99	31.89	17.69	9.04	33.09	17.37	28.49	39.57	47.55	55.53
	IFBDN	43.84	34.79	27.10	22.53	34.92	18.72	33.30	53.87	60.99	62.22
	PSDL	46.63	38.19	31.13	26.94	38.42	20.22	35.16	56.86	64.97	66.52
	CFPRF	66.34	55.47	48.05	40.96	55.22	18.48	35.57	58.06	65.47	66.53
	T3-Tracer	**68.74**	**57.28**	**49.25**	**42.73**	**57.28**	**21.65**	**37.36**	**59.64**	**66.47**	**67.30**

Table 3: Ablation study of effectiveness of our core modules.

Architecture	HAD		LAV-DF		PS	
	EER↓	mAP	EER↓	mAP	EER↓	mAP
Baseline=T3-Tracer	**0.07**	**99.27**	**0.80**	**94.29**	**7.41**	**57.28**
w/o. FFA	0.21	97.33	1.33	93.09	8.53	55.13
w/o. AFA	0.09	98.91	0.88	93.21	7.64	55.87
w/o. SMDAM	0.15	98.05	1.30	93.14	7.92	55.34

performance, as the network loses its ability to focus on abnormal cues. Finally, replacing gated fusion with simple addition reduces localization accuracy, validating the benefit of adaptive feature integration. Combining all three designs yields the best results.

Table 4: Ablation results on the internal mechanism of FA-FAM.

Architecture	HAD		LAV-DF		PS	
	EER↓	mAP	EER↓	mAP	EER↓	mAP
Baseline=FA-FAM	**0.07**	**99.27**	**0.80**	**94.29**	**7.41**	**57.28**
w/o. multi-core	0.08	98.14	0.96	93.23	7.94	56.59
w/o. anomaly gating	0.08	98.77	0.88	93.86	7.53	57.19
w/o. gate fusion	0.08	98.65	0.82	93.74	7.66	56.10

Ablation Study of the SMDAM. We examine three core designs in the local module: (1) modeling only original frame features, (2) modeling only frame differences, and (3) using a single-scale temporal segment. As shown in Table 5, either branch alone underperforms the full design, confirming that both the original and difference features capture complementary boundary cues. Moreover, using only a single temporal scale weakens sensitivity to forgery boundaries of varying durations. These results validate the necessity of dual-branch design and multi-scale modeling in capturing subtle local transitions.

Table 5: Ablation results on the internal mechanism of FA-FAM.

Architecture	HAD		LAV-DF		PS	
	EER↓	mAP	EER↓	mAP	EER↓	mAP
Baseline=SMDAM	**0.07**	**99.27**	**0.80**	**94.29**	**7.41**	**57.28**
w/o. frame features	0.08	98.59	0.85	93.88	7.65	56.71
w/o. frame differences	0.08	98.58	0.85	93.86	7.56	56.51
w/o. multi-scale temporal segment	0.08	98.16	0.98	93.21	7.83	56.19

Conclusion

In this paper, we proposed T3-Tracer, a unified framework for partial audio forgery detection and localization. A key contribution of our work is the explicit hierarchical temporal modeling, where we divide the temporal structure of audio into three levels: frame, segment, and audio. This multi-level decomposition enables a more comprehensive understanding of diverse forgery patterns. Based on this formulation, we designed two complementary modules: FA-FAM, which detects frame forgeries by integrating fine-grained acoustic cues at the frame level with global semantic context at the audio level; and SMDAM, which focuses on segment-level boundary detection by modeling original frame features and inter-frame differences across multi-scale segments. To enhance the interaction between temporal levels, we further introduced a cross-attention mechanism and a PRN-based decoder for coherent prediction. Extensive experiments on three challenging datasets demonstrate that T3-Tracer achieves state-of-the-art results on both Partial Forgery Detection and Temporal Forgery Localization. Our findings validate the importance of hierarchical temporal decomposition and cross-scale integration, offering a unified and extensible foundation for future progress in audio forgery detection under real-world and long-form scenarios.

References

Bińkowski, M.; Donahue, J.; Dieleman, S.; Clark, A.; Elsen, E.; Casagrande, N.; Cobo, L. C.; and Simonyan, K. 2019. High fidelity speech synthesis with adversarial networks. *arXiv preprint arXiv:1909.11646*.

Bodla, N.; Singh, B.; Chellappa, R.; and Davis, L. S. 2017. Soft-NMS–improving object detection with one line of code. In *Proceedings of the IEEE international conference on computer vision*.

Cai, Z.; Ghosh, S.; Adatia, A. P.; Hayat, M.; Dhall, A.; Gedeon, T.; and Stefanov, K. 2024. AV-Deepfake1M: A large-scale LLM-driven audio-visual deepfake dataset. In *Proceedings of the 32nd ACM International Conference on Multimedia*, 7414–7423.

Cai, Z.; Ghosh, S.; Dhall, A.; Gedeon, T.; Stefanov, K.; and Hayat, M. 2023. Glitch in the matrix: A large scale benchmark for content driven audio–visual forgery detection and localization. *Computer Vision and Image Understanding*.

Cai, Z.; and Li, M. 2024. Integrating frame-level boundary detection and deepfake detection for locating manipulated regions in partially spoofed audio forgery attacks. *Computer Speech & Language*.

Cai, Z.; Stefanov, K.; Dhall, A.; and Hayat, M. 2022. Do you really mean that? content driven audio-visual deepfake dataset and multimodal method for temporal forgery localization. In *2022 International Conference on Digital Image Computing: Techniques and Applications (DICTA)*.

Cai, Z.; Wang, W.; and Li, M. 2023. Waveform boundary detection for partially spoofed audio. In *ICASSP 2023-2023 IEEE International Conference on Acoustics, Speech and Signal Processing (ICASSP)*.

Conneau, A.; Baevski, A.; Collobert, R.; Mohamed, A.; and Auli, M. 2020. Unsupervised cross-lingual representation learning for speech recognition. *arXiv preprint arXiv:2006.13979*.

Eldele, E.; Ragab, M.; Chen, Z.; Wu, M.; and Li, X. 2024. Tslanet: Rethinking transformers for time series representation learning. *arXiv preprint arXiv:2404.08472*.

Gomez-Alanis, A.; Gonzalez-Lopez, J. A.; Dubagunta, S. P.; Peinado, A. M.; and Doss, M. M. 2020. On joint optimization of automatic speaker verification and anti-spoofing in the embedding space. *IEEE Transactions on Information Forensics and Security*.

Guo, Y.; Huang, H.; Chen, X.; Zhao, H.; and Wang, Y. 2024. Audio deepfake detection with self-supervised wavlm and multi-fusion attentive classifier. In *ICASSP 2024-2024 IEEE International Conference on Acoustics, Speech and Signal Processing (ICASSP)*.

Han, L.; Chen, X.-Y.; Ye, H.-J.; and Zhan, D.-C. 2024. Softs: Efficient multivariate time series forecasting with series-core fusion. *Advances in Neural Information Processing Systems*.

Huang, J.; Yuan, X.; Lam, C.-T.; Im, S.-K.; Lei, F.; and Bi, X. 2025. TransHFC: Joints Hypergraph Filtering Convolution and Transformer Framework for Temporal Forgery Localization. *IEEE Transactions on Circuits and Systems for Video Technology*.

Jung, J.-w.; Heo, H.-S.; Tak, H.; Shim, H.-j.; Chung, J. S.; Lee, B.-J.; Yu, H.-J.; and Evans, N. 2022. Aasist: Audio anti-spoofing using integrated spectro-temporal graph attention networks. In *ICASSP 2022-2022 IEEE international conference on acoustics, speech and signal processing (ICASSP)*, 6367–6371.

Kim, H.; Kim, S.; and Yoon, S. 2022. Guided-tts: A diffusion model for text-to-speech via classifier guidance. In *International Conference on Machine Learning*.

Li, D.; Tang, C.; and Liu, H. 2024. Audio-llm: Activating the capabilities of large language models to comprehend audio data. In *International Symposium on Neural Networks*.

Li, J.; Li, L.; Luo, M.; Wang, X.; Qiao, S.; and Zhou, Y. 2023. Multi-grained Backend Fusion for Manipulation Region Location of Partially Fake Audio. In *DADA@ IJCAI*.

Liu, M.; Wang, J.; Qian, X.; and Li, H. 2023. Audio-visual temporal forgery detection using embedding-level fusion and multi-dimensional contrastive loss. *IEEE Transactions on Circuits and Systems for Video Technology*.

Ma, W.; and Xia, G. 2024. Exploring the internal mechanisms of music llms: A study of root and quality via probing and intervention techniques. In *ICML 2024 Workshop on Mechanistic Interpretability*.

Ren, Y.; Hu, C.; Tan, X.; Qin, T.; Zhao, S.; Zhao, Z.; and Liu, T.-Y. 2020. Fastspeech 2: Fast and high-quality end-to-end text to speech.

Tak, H.; Patino, J.; Todisco, M.; Nautsch, A.; Evans, N.; and Larcher, A. 2021. End-to-end anti-spoofing with rawnet2. In *ICASSP 2021-2021 IEEE International Conference on Acoustics, Speech and Signal Processing (ICASSP)*.

Wang, C.; Yi, J.; Tao, J.; Sun, H.; Chen, X.; Tian, Z.; Ma, H.; Fan, C.; and Fu, R. 2022. Fully automated end-to-end fake audio detection. In *Proceedings of the 1st International Workshop on Deepfake Detection for Audio Multimedia*.

Wu, H.; Kang, J.; Meng, L.; Meng, H.; and Lee, H.-y. 2023. The defender's perspective on automatic speaker verification: An overview. *arXiv preprint arXiv:2305.12804*.

Wu, H.; Kuo, H.-C.; Zheng, N.; Hung, K.-H.; Lee, H.-Y.; Tsao, Y.; Wang, H.-M.; and Meng, H. 2022. Partially fake audio detection by self-attention-based fake span discovery. In *ICASSP 2022-2022 IEEE International Conference on Acoustics, Speech and Signal Processing (ICASSP)*.

Wu, J.; Lu, W.; Luo, X.; Yang, R.; Wang, Q.; and Cao, X. 2024. Coarse-to-fine proposal refinement framework for audio temporal forgery detection and localization. In *Proceedings of the 32nd ACM International Conference on Multimedia*.

Xie, Y.; Cheng, H.; Wang, Y.; and Ye, L. 2023. Domain generalization via aggregation and separation for audio deepfake detection. *IEEE Transactions on Information Forensics and Security*.

Xie, Y.; Cheng, H.; Wang, Y.; and Ye, L. 2024. An efficient temporary deepfake location approach based embeddings for partially spoofed audio detection. In *ICASSP 2024-2024 IEEE International Conference on Acoustics, Speech and Signal Processing (ICASSP)*.

Yi, J.; Bai, Y.; Tao, J.; Ma, H.; Tian, Z.; Wang, C.; Wang, T.; and Fu, R. 2021. Half-truth: A partially fake audio detection dataset.

Zhang, C.-L.; Wu, J.; and Li, Y. 2022. Actionformer: Localizing moments of actions with transformers. In *European Conference on Computer Vision*.

Zhang, K.; Hua, Z.; Lan, R.; Guo, Y.; Zhang, Y.; and Xu, G. 2025. Multi-View Collaborative Learning Network for Speech Deepfake Detection. In *Proceedings of the AAAI Conference on Artificial Intelligence*.

Zhang, L.; Wang, X.; Cooper, E.; Evans, N.; and Yamagishi, J. 2022. The partialspoof database and countermeasures for the detection of short fake speech segments embedded in an utterance. *IEEE/ACM Transactions on Audio, Speech, and Language Processing*.

Zhang, R.; Wang, H.; Du, M.; Liu, H.; Zhou, Y.; and Zeng, Q. 2023. Ummaformer: A universal multimodal-adaptive transformer framework for temporal forgery localization. In *Proceedings of the 31st ACM International Conference on Multimedia*.

Zhou, Q.; Pei, C.; Sun, F.; Han, J.; Gao, Z.; Pei, D.; Zhang, H.; Xie, G.; and Li, J. 2024. Kan-ad: time series anomaly detection with kolmogorov-Arnold networks. *arXiv preprint arXiv:2411.00278*.

Zhou, Z.; Zhou, J.; Qian, W.; Tang, S.; Chang, X.; and Guo, D. 2025. Dense audio-visual event localization under cross-modal consistency and multi-temporal granularity collaboration. In *Proceedings of the AAAI Conference on Artificial Intelligence*.

Zhu, Y.; Chen, Y.; Zhao, Z.; Liu, X.; and Guo, J. 2023. Local self-attention-based hybrid multiple instance learning for partial spoof speech detection. *ACM Transactions on Intelligent Systems and Technology*.

Zou, H.; Shen, M.; Hu, Y.; Chen, C.; Chng, E. S.; and Rajan, D. 2024. Cross-modality and within-modality regularization for audio-visual deepfake detection. In *ICASSP 2024-2024 IEEE International Conference on Acoustics, Speech and Signal Processing (ICASSP)*.